A&A manuscript no.
(will be inserted by hand later)

Your thesaurus codes are:
06; 19.63.1

ASTRONOMY AND ASTROPHYSICS

A Cannonball model of γ-ray bursts: spectral and temporal properties of the γ-rays

Arnon Dar[1,2] **and A. De Rújula**[1]

1. Theory Division, CERN, CH-1211 Geneva 23, Switzerland
2. Physics Department and Space Research Institute, Technion, Haifa 32000, Israel

the date of receipt and acceptance should be inserted later

arXiv:astro-ph/0012227v1 11 Dec 2000

Abstract. Recent observations suggest that gamma ray bursts (GRBs) and their afterglows are produced by highly relativistic jets emitted in supernova explosions. We have proposed that the result of the event is not just a compact object plus the ejecta: within days, a fraction of the parent star falls back to produce a thick accretion disk. The subsequent accretion generates jets and constitutes the GRB "engine", as in the observed ejection of relativistic "cannonballs" of plasma by microquasars and active galactic nuclei. Here we investigate the production of a GRB as the jetted cannonballs exit the supernova shell reheated by their collision with it, emitting highly forward-collimated radiation. Each cannonball corresponds to an individual pulse in a GRB. We cannot predict the timing sequence of these pulses, but the Cannonball Model fares very well in describing the total energy, energy spectrum, and time-dependence of the individual pulses.

Key words: gamma rays bursts, supernovae, black holes

1. Introduction

Once upon a time, Gamma Ray Bursts (GRBs) constituted a sheer mystery, whose unassailability was reflected in the scores of extremely different ideas proposed to explain them. In spite of giant strides in the recent observations —the discovery of GRB afterglows (Costa et al. 1997; van Paradijs et al. 1997), the discovery of the association of GRBs with supernovae (Galama et al. 1998), and the measurements of the reedshifts of their host galaxies (Metzger et al. 1997)— the origin of GRBs is still an unresolved enigma. In the recent past, the generally accepted view has been that GRBs are generated by synchrotron emission from fireballs, or firecones, produced by collapses or mergers of compact stars (Paczynski 1986; Goodman et al. 1987; Meszaros and Rees 1992) by failed supernovae or collapsars (Woosley 1993; Woosley and MacFadyen 1999; MacFadyen and Woosley 1999, Woosley 1999) or by hypernova explosions (Paczynski 1998). But various observations suggest that most GRBs are produced in supernova events by highly collimated ultrarelativistic jets (Shaviv and Dar 1995; Dar 1998; Dar and Plaga 1999; Cen 1999; Dar and De Rújula 2000a and references therein).

In a previous paper (Dar and De Rújula 2000a) we introduced a relativistic-cannonball model in which GRBs are produced by "cannonballs" (CBs) of baryonic plasma emitted subsequently to a core-collapse supernova (SN) explosion, and are observable when they happen to point close to our direction. There, we concentrated on GRB afterglows —due to bremsstrahlung and synchrotron emission from the CBs after they become transparent to their own enclosed radiation— to emphasize how, in the case of GRB 980425, it might be possible to observe the CBs' "superluminal" motion. In this paper we briefly review the CB model and we derive its predictions for the properties of the γ-rays in a GRB, generated as the forward-collimated and blue-shifted thermal radiation from a succession of fast-moving, cooling and expanding CBs — previously heated by their collision with the SN shell— escapes from the transparent outer regions of the shell. We study the γ-ray distributions in time, their energy-spectrum and the correlations between these two observables, showing that the CB model explains the main observed features of GRBs.

2. Jets in astrophysics

Relativistic jets seem to be emitted by all astrophysical systems wherein mass is accreted at a high rate from a disk onto a central compact object (for a review, see Mirabel and Rodriguez 1999a). Highly relativistic jets have been observed in galactic sources, such as the microquasars GRS 1915+105 (Mirabel and Rodriguez 1994, 1999a,b; Rodriguez and Mirabel 1999) and GRO J165-40 (Tingay et al. 1995) where mass is accreted onto a stellar black hole, and in many active galactic nuclei hosting a massive black hole. These jets are not continuous streams: they consist of individual blobs of plasma (plasmoids or cannonballs), and their firing coincides with a sudden removal of the accretion-disk material (Belloni 1997; Mirabel and Rodriguez 1999b). Cannonballs in microquasars –and presumably also in quasars– are emitted in pairs, moving in opposite directions.

As they travel, microquasar CBs are observed to expand at a speed comparable to, or smaller than, the sound speed of a relativistic plasma ($c/\sqrt{3}$ in their rest system) probably because the energy density of their enclosed radiation is comparable to that of their matter constituency. As they become transparent and cool down, the CBs' lateral size stabilizes to a roughly constant value, presumably constrained by magnetic self-containment and/or by the ram pressure of the ambient material. Quasar CBs show no measurable expansion as they travel, sometimes for as long as a million light years (see, e.g., Bridle 2000; Wilson et al. 2000). Galactic and quasar CBs expand explosively when finally stopped by the material they traverse.

3. The cannonball model of GRBs

The ejection of matter in a supernova (SN) explosion is not fully understood. The known mechanisms for imparting the required kinetic energy to the ejecta are inefficient: the theoretical understanding of core-collapse SN events is still unsatisfying. It has been proposed (De Rújula 1987; Woosley 1993, Dar and De Rújula 2000a and references therein) that the result of a SN event is not just a compact object plus the ejecta: a fraction of the parent star may be ejected, but another fraction of its mass may fall back onto the newly born compact object. For vanishing angular momentum, the free-fall time of a test-particle from a parent stellar radius $R_\star$ onto an object of mass M_c is:

$$t_{\rm fall} = \pi \left[\frac{R_\star^3}{8\,G\,M_c}\right]^{1/2} \sim 1\ {\rm day}\ \left[\frac{R_\star}{10^{12}\ {\rm cm}}\right]^{3/2}\ \left[\frac{1.4\ M_\odot}{M_c}\right]^{1/2}. \quad (1)$$

The free-fall time is shorter if the mass of the falling material is not small relative to that of the compact object. The fall-time is longer (except for material falling from the polar directions) if the specific angular momentum is considerably large, as it is in most stars. The estimate of Eq.(1) is therefore a rough one.

It is quite natural to suppose that infalling material with non-vanishing angular momentum settles into an orbiting disk, or a thick torus if its mass is comparable to M_c. We assume that, as observed in other cases of significant accretion onto a compact object (microquasars and active galactic nuclei) in which the infalling material is processed in a series of "catastrophic" accretions, jets of relativistic CBs of plasma are ejected. We presume their composition to be "baryonic", as it is in the jets of SS 433, from which Ly_α and Fe K_α lines have been detected (Margon 1984), although the violence of the relativistic jetting-process should in our case break most nuclei into their constituents.

The mechanism producing relativistic jets in accretion processes and its timing-sequence are not understood (for suggested possibilities see, e.g., Blandford and Znajek 1977; Meszaros and Rees 1997). In our model we assume that a series of CBs is ejected, each one giving rise to one of the "pulses" of a specific GRB. After a few pulses the engine runs out of fuel, and the γ-ray activity ceases. The timing sequence of the successive pulses we are unable to predict, but, as we shall show, the CB model is quite successful in describing the time-dependence of the γ-ray flux *within single GRB pulses*.

In brief, the CB model is the following. A sequence of oppositely-directed pairs of cannonballs is emitted at a time $t_{\rm fall}$ of $\mathcal{O}(1)$ day after a SN core-collapse. By this time the SN outer shell, traveling at a velocity $v_S \sim c/10$ (see, e.g., Nakamura et al. 2000) has moved to a distance:

$$R_S = 2.6\times10^{14}\ {\rm cm}\ \left(\frac{t_{\rm fall}}{1\ {\rm d}}\right)\ \left(\frac{10\,v_S}{c}\right). \quad (2)$$

We adopt $R_S = 2.6\times10^{14}$ cm as a "reference" value, to which our results will be scaled. The reference values of various relevant parameters —that serve as bench-marks to which to scale our results and imply no strong commitment to their particular choices— are listed in Table I, for quick reference. We denote with a bar the actual value of a parameter in the units of its reference value so that $\overline{R}_S$, for instance, means a given SN-shell radius divided by 2.6×10^{14} cm.

Only if traveling at a small angle θ relative to the line of sight, will a CB be visible. As it hits the SN shell, the CB slows down and heats up. Its radiation is obscured by the shell up to a distance of order one radiation length from the shell's outer surface. As this point is reached, the GRB is emitted by a CB that continues to travel, expand and cool down, its radiation being boosted and collimated by the CB's ultrarelativistic motion. We do not discuss in this paper the GRB afterglows (Dar and De Rújula 2000a), the flash of X-ray lines and the achromatic flare in the afterglow as the electrons and protons in the GRB recombine (Dar and De Rújula 2000b), nor the flux of high energy neutrinos and γ-rays produced by the decays of pions made in the CB's collision with the SN shell (Dar and De Rújula 2000c).

There are other events in which a variety of GRBs could be produced by mechanisms similar to the ones we have discussed: large mass accretion episodes in binaries including a compact object, mergers of neutron stars with neutron stars or black holes (Paczynski 1986, Goodman et al. 1987), transitions of neutron stars to hyperon- or quark-stars (Dar 1999; Dar and De Rújula, 2000d), etc. In each case, the ejected cannonballs would make GRBs by hitting stellar winds or envelopes, circumstellar mass or light. We discuss only core-collapse SN explosions, as the GRBs they would produce by our mechanism, although relatively "standard", satisfactorily reproduce the general properties of the heterogeneous ensemble of GRBs.

4. Four "clocks" and three energy scales

Let $\gamma = 1/\sqrt{1-\beta^2} = \mathrm{E_{CB}}/(\mathrm{M_{CB}c^2})$ be the Lorentz factor of a CB, that diminishes with time as the CB hits the SN shell and as it subsequently plows through the interstellar medium. Four clocks ticking at different paces are relevant to a CB's history. Let $\mathrm{t_{SN}}$ be the local time in the SN rest system, $\mathrm{t_{CB}}$ the time in the CB's rest system, $\mathrm{t_{Ob}}$ the time measured by a nearby observer viewing the CB at an angle θ away from its direction of motion and t the time measured by an earthly observer viewing the CB at the same angle, but from a "cosmological" distance (redshift $\mathrm{z} \neq 0$). Let x be the distance traveled by the CB in the SN rest system. The relations between the above quantities are:

$$\mathrm{dt_{SN}} = \gamma\,\mathrm{dt_{CB}} = \frac{\mathrm{dx}}{\beta\,\mathrm{c}}\,;$$
$$\mathrm{dt_{CB}} \equiv \delta\,\mathrm{dt_{Ob}}\,;\;\; \mathrm{dt} = (1+\mathrm{z})\,\mathrm{dt_{Ob}}\,, \tag{3}$$

where the Doppler factor δ is:

$$\delta \equiv \frac{1}{\gamma\,(1-\beta\cos\theta)} \simeq \frac{2\,\gamma}{(1+\theta^2\gamma^2)}\,, \tag{4}$$

and its approximate expression is valid for $\theta \ll 1$ and $\gamma \gg 1$, the domain of interest here. Notice that for large γ and $\theta\gamma$ not large, there is an enormous "relativistic aberration": $\mathrm{dt} \sim \mathrm{dt_{SN}}/\gamma^2$ and the observer sees a long CB story as a film in extremely fast motion.

The energy of the photons radiated by a CB in its rest system, $\mathrm{E^{\gamma}_{CB}}$, their energy in the direction θ in the local SN system, $\mathrm{E^{\gamma}_{SN}}$, and the photon energy, E, measured by a cosmologically distant observer, are related by:

$$\mathrm{E^{\gamma}_{CB}} = \frac{\mathrm{E^{\gamma}_{SN}}}{\delta}\,;\;\; \mathrm{E^{\gamma}_{SN}} = (1+\mathrm{z})\,\mathrm{E}\,, \tag{5}$$

with δ as in Eq.(4).

5. The making of a GRB

5.1. Jet energy and CB mass

Let "jet" stand for the ensemble of CBs emitted in one direction in a SN event. If a momentum imbalance between the opposite-direction jets is responsible for the large peculiar velocities $\mathrm{v_{NS}} \approx 450 \pm 90$ km s^{-1} (Lyne and Lorimer 1994) of neutron stars born in SNe, the jet kinetic energy $\mathrm{E_{jet}}$ must be, as we shall assume for our GRB engine, larger than $\sim 10^{52}$ erg (e.g. Dar and Plaga 1999). The jet-emitting process may be "up-down" symmetric to a very good approximation, in which case the jet energies may be much bigger. There is evidence that in the accretion of matter by black holes in quasars (Celotti at al. 1997; Ghisellini 2000) and microquasars (Mirabel and Rodriguez 1999a,b) the efficiency for the conversion of gravitational binding energy into jet energy is surprisingly large. If in the production of CBs the central compact object in a SN ingurgitates several solar masses, it is not out of the question that $\mathrm{E_{jet}}$ be as large as $\mathrm{M_{\odot}c^2} \sim 1.8 \times 10^{54}$ erg. We shall adopt here a compromise value, 10^{53} ergs, as the reference jet energy.

Let γ_{in} be the Lorentz factor of a cannonball as it is fired. Let $\mathrm{E_{CB}} = \mathrm{f\,E_{jet}}$ be the energy of a CB; on average GRBs have some five to ten significant pulses, so that the fraction f may typically be 1/5 or 1/10. We shall adopt $\mathrm{E_{CB}} = 10^{52}$ erg as our reference value. For this value, the CB's mass is comparable to an Earth mass: $\mathrm{M_{CB}} \sim 1.8\,\mathrm{M_{\otimes}}(10^3/\gamma_{\mathrm{in}})$, for a Lorentz factor of $\gamma_{\mathrm{in}} = \mathcal{O}(10^3)$, that we shall find to be "typical".

5.2. CB deceleration by the SN shell

Let $\beta_{\mathrm{in}}\,\mathrm{c}$ be the expansion velocity of a CB, in its rest system, as it travels from the point of emission to the point at which it reaches the SN shell. For the reference value of β_{in}, as reported in Table I, we use $1/(10\sqrt{3})$: one tenth of the sound velocity of a relativistic plasma. The CB reaches the shell with a radius

$$\mathrm{R_{CB}} \sim \mathrm{R_S}\,\frac{\beta_{\mathrm{in}}}{\gamma_{\mathrm{in}}} \tag{6}$$

and sweeps up a "target" mass $\mathrm{M_T} \sim \pi\,\mathrm{R^2_{CB}}\,\mathrm{X_S} = \mathrm{M_S}\,\beta^2_{\mathrm{in}}/(4\,\gamma^2_{\mathrm{in}})$, or some $\sim 2.8 \times 10^{-3}\,\mathrm{M_{\otimes}}$, for our reference parameter values and $\gamma_{\mathrm{in}} = 10^3$. The CB and the SN shell are "thick" in the sense of extending over many radiation lengths and many nucleon-nucleon interaction lengths. A high-energy nucleon suffering successive interactions in a dilute gas or plasma loses roughly 2/3 of its energy to $\pi^{\pm}$ production, with most of the pion energy being carried away by the neutrinos in $\pi \to \mu\,\nu$ decays and the subsequent μ decays. The electrons from μ decay and the photons from π^0 decay locally deposit roughly 1/3 of the original nucleon energy.

The Lorentz factor of the CB after it has swept the SN shell, γ_{out}, is simply the ratio of the total energy to the invariant mass ($\sqrt{\mathrm{s}} = \mathrm{M\,c^2}$) of the outgoing object:

$$\gamma_{\mathrm{out}} \simeq \frac{\mathrm{E_{CB}}/3}{\sqrt{\mathrm{s}}} \simeq \frac{\mathrm{E_{CB}}/3}{\sqrt{2\,\mathrm{M_T\,c^2\,E_{CB}}/3 + \mathrm{M^2_{CB}\,c^4}}}\,, \tag{7}$$

where we have used $\mathrm{E_{CB}} \gg \mathrm{M_T c^2}$. Substituting for $\mathrm{M_T}$ and $\mathrm{M_{CB}}$ as functions of γ_{in} and β_{in}, one obtains:

$$\gamma_{\mathrm{out}} \simeq \gamma_{\mathrm{in}}\,\sqrt{\frac{2\,\mathrm{E_{CB}}}{3\,\beta^2_{\mathrm{in}}\,\mathrm{M_S\,c^2} + 18\,\mathrm{E_{CB}}}} \tag{8}$$

whose limiting values are:

$$\gamma_{\mathrm{out}} \sim \frac{\gamma_{\mathrm{in}}}{3} \quad (\mathrm{for}\; 6\,\mathrm{E_{CB}} \gg \beta^2_{\mathrm{in}}\,\mathrm{M_S\,c^2})\,,$$
$$\gamma_{\mathrm{out}} \sim \frac{\gamma_{\mathrm{in}}}{3\,\overline{\beta}_{\mathrm{in}}}\,\left[\frac{\overline{\mathrm{E}}_{\mathrm{CB}}}{\overline{\mathrm{M}}_{\mathrm{S}}}\right]^{\frac{1}{2}} \quad (\mathrm{for}\; 6\,\mathrm{E_{CB}} \ll \beta^2_{\mathrm{in}}\,\mathrm{M_S\,c^2})\,. \tag{9}$$

For our reference $\gamma_{\mathrm{out}} \sim 10^3$, the values of γ_{in} implied by Eqs.(9) may look surprisingly large. But Eqs.(9) do not

depend on R_S: any relativistic jet exiting from the core of a SN encounters the same amount of non-collapsed material, and must have a γ_{in} considerably larger than γ_{out}.

The very large value of γ_{in} ($\sim 3\times10^3$ for our reference parameters) implies that the fractional solid angle covered by a CB as it hits the SN shell is tiny: $\beta_{in}^2/(4\,\gamma_{in}^2) \sim 10^{-10}$, again for our reference parameters. This presumably makes it unlikely for successive CBs to hit precisely the same spot in the SN shell: CB-CB collisions and mergers may be the exception, rather than the rule.

5.3. Attenuation of the γ rays

The density profile of the outer layers of a SN shell as a function of the distance x to the SN center can be measured from the photometry, spectroscopy and evolution of the SN emissions (see e.g. Nakamura et al. 2000 and references therein). The observations can be fit by a power law, x^{-n}, with $n \sim 4$ to 8. Our results are sensitive to this density profile only in the outer region where the SN shell becomes transparent (and the measurements are made), so that we can adopt the same profile at all $x > R_S$:

$$\rho(x) = \rho(R_S)\,\Theta(x-R_S)\,\left[\frac{R_S}{x}\right]^n . \qquad (10)$$

The SN-shell grammage still in front of a CB located at x is:

$$X_S(x) = \int_x^\infty \rho(y)\,dy = \frac{M_S}{4\,\pi\,R_S^2}\,\left[\frac{R_S}{x}\right]^{n-1} . \qquad (11)$$

For photons in the MeV domain the attenuation length is similar, within a factor 2, in all elements from H to Fe (Groom et al., 2000), and can be roughly approximated by:

$$X_\gamma(E) \sim 1.0\,(E/\mathrm{keV})^{0.33}\ \mathrm{g\,cm^{-2}} . \qquad (12)$$

The value of $X_\gamma(E)$ in the E = 10 keV to 1 MeV domain (2.1 to 9.8 gr/cm^2) is close to the attenuation length in a hydrogenic plasma ($X_\gamma^{ion} \simeq m_p/\sigma_T \simeq 2.6$ gr/cm^2, with m_p the proton's mass and $\sigma_T \simeq 0.65\times10^{-24}$ cm^2 the Thomson cross-section). Therefore, it makes little difference in practice whether or not we take into account that the SN-shell material reached by the CB may be ionized by its previously emitted radiation. Equating $X_S(x) = X_\gamma(E)$ and solving for x, we define a useful quantity: $x_{tp}(E)$, the position at which the SN shell becomes (one-radiation-length) transparent:

$$x_{tp}(E) = R_S\,\left[\frac{M_S}{4\,\pi\,R_S^2}\,\frac{1}{X_\gamma(E)}\right]^{\frac{1}{n-1}} \propto E^{-0.33/(n-1)} , \qquad (13)$$

whose energy dependence is extremely weak. Blue-shifted to the SN rest-system, as in Eq.(5), GRB photons have energies in the MeV range. Let $\tilde{x}_{tp} \equiv x_{tp}(1\ \mathrm{MeV})$. For our reference parameters, some representative results are: $\tilde{x}_{tp} \simeq 2.9\,R_S$ for n = 8, $\tilde{x}_{tp} \simeq 4.5\,R_S$ for n = 6. At $\tilde{x}_{tp}$, $\rho(x)$ is orders of magnitude smaller than at $x \sim R_S$, where most of the SN-shell's mass is steeply concentrated. This will simplify our discussion, for it is a fair approximation to have the CB slow down at heat up close to $x = R_S$, and proceed thereafter unperturbed by the SN-shell material, except inasmuch as little of its radiation can escape before it reaches $x = \tilde{x}_{tp}$. At that point, the CB has expanded from the radius R_{CB} of Eq.(6) to a radius at transparency:

$$R_{CB}^{tp} \simeq R_{CB} + \frac{\tilde{x}_{tp}-R_S}{\gamma_{out}}\,\beta_{out} \simeq \frac{\tilde{x}_{tp}-R_S}{\gamma_{out}}\,\beta_{out} , \qquad (14)$$

some 2.9×10^{11} cm, for our reference parameters. The CB itself becomes transparent to the radiation it encloses later, when it reaches a radius $\widetilde{R}_{CB}^{tp} \simeq [3\,M_{CB}\,\sigma_T/(4\,\pi\,m_p)]^{\frac{1}{2}}$. We expect the CB to stop expanding at a proper quasi-relativistic rate β_{out} soon after it becomes transparent and its inner radiation pressure drops abruptly: the inertial mildly relativistic transverse motion of its matter constituents is slowed-down by interstellar material and, perhaps, by self-confining magnetic fields.

5.4. Total energy of a GRB pulse

A CB expanding as a quasi-relativistic plasma ought to reach the SN shell with a shape (in its rest system) very close to spherical. The microscopic description of what happens as the CB and the material of the SN shell collide and coalesce is elaborate (Dar and De Rújula, 2000c). Much of the available energy is deposited at the CB's front surface by nucleons sharing their energy and γ's from π^0-decay depositing theirs. Electrons from μ decay deposit their energy much deeper into the CB. The ionized CB's material is hot and dense enough for the deposited energy to thermalize very fast. As it impinges the SN shell, a CB may have a tendency to get flattened, but the velocities, $\beta \approx 1-1/(2\gamma^2)$, corresponding to γ_{in} and γ_{out} are so similar that no significant flattening occurs between the time the CB hits the shell and the time it reaches the point at which the shell becomes transparent to the CB's radiation: flattening is subdominant relative to the CB's expansion. For the subsequent estimates we approximate the CB as a spherical body with a uniform internal temperature.

The proper temperature T_0 acquired by the CB as it hits the SN shell is high enough for the CB's internal-radiation energy-density to be much larger than the mass-energy density of its matter constituents. Consequently, T_0 can be estimated by equating the total internal radiation energy to the invariant mass in the CB-SN shell collision:

$$T_0 \simeq \left[\frac{3}{8\,\pi\,a}\,\sqrt{\frac{3}{2}}\,\frac{(3\,\beta_{in}^2\,M_S\,c^2+18\,E_{CB})^{3/2}}{\sqrt{E_{CB}}}\,\frac{\gamma_{out}^2}{R_S^3}\right]^{\frac{1}{4}} , \qquad (15)$$

where $a \simeq 1.37\times10^{14}$ erg cm^{-3} keV^{-4} is the radiation-density constant. The result, $T_0 \sim 3.4$ keV for our refer-

ence parameters, is very insensitive to their values, but for the $R_S^{-3/4}$ dependence on the SN-shell's radius.

Since the SN-shell's material is highly concentrated close to $x = R_S$, as in Eq.(11), we can take T_0 to be the temperature at that point. A rough estimate of the total energy in a GRB pulse can be obtained as follows. While on the part of the shell that is not transparent, the CB does not lose much energy via surface radiation, so that it expands quasi-adiabatically at roughly constant $R_{CB}(t)\,T(t)$. At the point at which the shell becomes transparent, the internal-radiation energy in the CB is reduced, from the value $\sqrt{s}$ of Eq.(7), to $E_{tp} \simeq \sqrt{s}\; R_{CB}/R^{tp}_{CB}$. Approximately 1/e of this energy is emitted thereafter, its value in the CB's rest system is:

$$E^{rest}_{pulse} \simeq \frac{1}{3\,e}\,\frac{E_{CB}}{\gamma_{in}}\,\frac{R_S}{\tilde{x}_{tp}-R_S}\,\frac{\beta_{in}\,\gamma_{out}}{\beta_{out}\,\gamma_{in}}\,, \tag{16}$$

whose limiting values are:

$$E^{rest}_{pulse} \simeq 4.5\times10^{45}\ \text{erg}\,\left[\frac{3\,R_S}{\tilde{x}_{tp}-R_S}\right]\,\frac{1}{\overline{\gamma}_{out}}\,\frac{\overline{\beta}_{in}}{\overline{\beta}_{out}}$$
$$(\text{for } 6\,E_{CB} \gg \beta^2_{in}\,M_S\,c^2)\,,$$
$$E^{rest}_{pulse} \simeq 4.5\times10^{45}\ \text{erg}\,\left[\frac{3\,R_S}{\tilde{x}_{tp}-R_S}\right]\,\frac{1}{\overline{\gamma}_{out}\,\overline{\beta}_{in}\,\overline{\beta}_{out}}\,\frac{\overline{E}^2_{CB}}{\overline{M}_S}$$
$$(\text{for } 6\,E_{CB} \ll \beta^2_{in}\,M_S\,c^2)\,. \tag{17}$$

An observer at rest, located at a known luminosity distance $D_L(z)$ from the CB and viewing it at an angle θ from its direction of motion would measure a "total" (time- and energy-integrated) fluence per unit area:

$$\frac{dF}{d\Omega} \simeq \frac{1+z}{4\,\pi\,D^2_L}\,E^{rest}_{pulse}\;\delta^3\,, \tag{18}$$

where $\delta = \delta[\gamma,\theta]$ is given, here and in what follows, by Eq.(4) with $\gamma = \gamma_{out}$. The "spherical" energy deduced from this result would be an overestimate of the true energy E^{rest}_{pulse} by the last factor in Eq.(18), which, for $\gamma_{out} = 10^3$ and $\theta\gamma \sim \mathcal{O}(1)$, can be as large as $\sim 10^9$. Enhanced by a factor ranging up to this large number, the GRB-pulse energies of Eq.(16) can easily reproduce the observations, as discussed in detail in Section 7.

Armed with an expression such as Eq.(18) one can embark in the exercise of studying the extent to which GRBs are standard candles, by checking whether the observations at fixed redshift are statistically compatible with this expression for a uniformly distributed $\cos\theta$ distribution. But the current number of GRBs with measured redshifts is only fifteen, and their deduced total energies are affected by absorption, by experimental efficiency and threshold effects, etc. We do not, in this paper, attempt such an analysis, that has been initiated, with encouraging results, by Plaga (2000), who uses —to extract redshifts from a large collection of GRBs— the "Cepheid-like" relationship between variability and luminosity proposed by Fenimore and Ramirez-Ruiz (2000).

5.5. Energy and time dependence of a γ-ray pulse

A CB, as it reaches the transparent outskirts of a SN shell, is expanding and cooling and its radiation is becoming visible to the observer. In what follows it is convenient to measure the GRB observer's time, t, setting $t = 0$ at the moment of the encounter of the CB and the SN shell. The time of (one-radiation-length) transparency is then:

$$t_{tp} \simeq \frac{1+z}{\gamma_{out}\,\delta}\,\frac{\tilde{x}_{tp}-R_S}{c}\,. \tag{19}$$

The CB temperature at $t = t_{tp}$ is:

$$T_{tp} \sim \left[\frac{3}{4\,\pi\,a}\,\frac{E^{rest}_{pulse}}{(R^{tp}_{CB})^3}\right]^{\frac{1}{4}}\,, \tag{20}$$

whose limiting values are:

$$T_{tp} \sim 0.1\ \text{keV}\left[\frac{3\,R_S}{\tilde{x}_{tp}-R_S}\right]\,\frac{\overline{\gamma}^{\frac{1}{2}}_{out}\,\overline{\beta}^{\frac{1}{4}}_{in}}{\overline{\beta}_{out}}$$
$$(\text{for } 6\,E_{CB} \gg \beta^2_{in}\,M_S\,c^2)\,,$$
$$T_{tp} \sim 0.1\ \text{keV}\left[\frac{3\,R_S}{\tilde{x}_{tp}-R_S}\right]\,\frac{\overline{\gamma}^{\frac{1}{2}}_{out}}{\overline{\beta}^{\frac{1}{4}}_{in}\,\overline{\beta}_{out}}\,\frac{\overline{E}^{\frac{1}{2}}_{CB}}{\overline{M}^{\frac{1}{4}}_S}$$
$$(\text{for } 6\,E_{CB} \ll \beta^2_{in}\,M_S\,c^2)\,. \tag{21}$$

The time-dependences of the CB's radius, its temperature, and the distance x of the CB from the SN's center are, for $t > 0$:

$$R_{CB}[t] \simeq R_{CB} + R^{tp}_{CB}\,\frac{t}{t_{tp}} \sim R^{tp}_{CB}\,\frac{t}{t_{tp}}\,,$$
$$T[t] \simeq T_{tp}\,\frac{R^{tp}_{CB}}{R_{CB}[t]}\,,$$
$$x[t] \simeq R_S + \frac{\delta\,\gamma_{out}}{1+z}\,c\,t\,. \tag{22}$$

Let the number of photons per unit time and energy, assumed to be isotropically emitted by the CB in its rest system, be:

$$\frac{dn_\gamma}{dE_\gamma\,dt_{CB}} \equiv F(E^\gamma_{CB}, T)\,. \tag{23}$$

Using Eqs.(3-5) to change variables to E and t (the γ-ray energy and time in the observer's frame), we obtain:

$$\frac{dn_\gamma}{dE\,dt} \simeq F\left(E\,\frac{1+z}{\delta}, T[t]\right)\,. \tag{24}$$

In the approximation in which the CB's emission in its rest system is a thermal distribution from its surface, the function F is:

$$F(E^\gamma_{CB}, T) \simeq \frac{2\,\pi\,\sigma}{\zeta(3)}\,(R_{CB}[t])^2\,\frac{(E^\gamma_{CB})^2}{\text{Exp}\{E^\gamma_{CB}/T\}-1}\,, \tag{25}$$

where $\sigma = c\,a/4$ is the Stefan-Boltzmann constant.

The observed energy and time dependence of the photon intensity (photon number per unit area, N) of a single pulse in a GRB at an angle θ relative to the CB's motion is then predicted to be:

$$\frac{\mathrm{dN}}{\mathrm{dE\,dt}} \equiv \frac{1+\mathrm{z}}{4\,\pi\,\mathrm{D_L^2}}\,\delta^2\,\frac{\mathrm{dn}_\gamma}{\mathrm{dE\,dt}}\,, \tag{26}$$

$$\frac{\mathrm{dn}_\gamma}{\mathrm{dE\,dt}} \simeq \frac{2\,\pi\,\sigma}{\zeta(3)}\,\frac{[\mathrm{R_{CB}[t]\,E\,(1+z)}/\delta]^2\;\mathrm{Abs(E,t)}}{\mathrm{Exp\,\{E\,(1+z)/(\delta\,T[t])\}}-1}\,, \tag{27}$$

with $\mathrm{R_{CB}[t]}$ and $\mathrm{T[t]}$ as in Eqs.(22), and where

$$\mathrm{Abs(E,t)} = \mathrm{Exp}\left[-\frac{\mathrm{X_S(x[t])}}{\mathrm{X_\gamma(E\,(1+z))}}\right] \tag{28}$$

is the attenuation of the flux in the SN shell.

For n in Eq.(13) as large as the observations indicate ($\mathrm{n}\sim 6$), the absorption factor $\mathrm{Abs(E^\gamma,t)}$ rises very sharply from 0 to 1 around $\mathrm{t}=\mathrm{t_{tp}}$, in which case the width of a GRB pulse in energy and time is governed by the exponential in the denominator of Eq.(27). The argument of that exponential can be simply rewritten as $\mathrm{E\,t/H}$, with:

$$\mathrm{H} \equiv \frac{\tilde{\mathrm{x}}_{\mathrm{tp}}-\mathrm{R_S}}{\mathrm{c}\,\gamma_{\mathrm{out}}}\,\mathrm{T_{tp}}\,, \tag{29}$$

whose limiting values are:

$$\begin{aligned}\mathrm{H} &\sim 2.5\ \mathrm{keV\,s}\ \frac{\overline{\beta}_{\mathrm{in}}^{\frac{1}{4}}}{\overline{\gamma}_{\mathrm{out}}^{\frac{1}{2}}\,\overline{\beta}_{\mathrm{out}}}\\ &\qquad(\mathrm{for}\ 6\,\mathrm{E_{CB}} \gg \beta_{\mathrm{in}}^2\,\mathrm{M_S\,c^2})\,,\\ \mathrm{H} &\sim 2.5\ \mathrm{keV\,s}\ \frac{1}{\overline{\gamma}_{\mathrm{out}}^{\frac{1}{2}}\,\overline{\beta}_{\mathrm{out}}\,\overline{\beta}_{\mathrm{in}}^{\frac{1}{4}}}\ \frac{\overline{\mathrm{E}}_{\mathrm{CB}}^{\frac{1}{2}}}{\overline{\mathrm{M}}_{\mathrm{S}}^{\frac{1}{4}}}\\ &\qquad(\mathrm{for}\ 6\,\mathrm{E_{CB}} \ll \beta_{\mathrm{in}}^2\,\mathrm{M_S\,c^2})\,.\end{aligned} \tag{30}$$

6. Some simplifications and approximate correlations

To guide the eye, we give a simplified approximate form of Eq.(13), which we do not use in our explicit calculations:

$$\frac{\mathrm{dN}}{\mathrm{dE\,dt}} \propto \frac{(\mathrm{E\,t})^2}{\mathrm{Exp\{E\,t/H\}}-1}\,\mathrm{Exp}\left\{-\left[\mathrm{t_{tp}/t}\right]^{\mathrm{n}-1}\right\}\,\Theta[\mathrm{t}]\,. \tag{31}$$

The total photon intensity and energy flux are, in this approximation:

$$\frac{\mathrm{dN}}{\mathrm{dt}} \propto \Theta[\mathrm{t}]\,\frac{\mathrm{t_{tp}}}{\mathrm{t}}\,\mathrm{Exp}\left\{-\left[\mathrm{t_{tp}/t}\right]^{\mathrm{n}-1}\right\}\,, \tag{32}$$

$$\mathrm{F_E(t)} \propto \Theta[\mathrm{t}]\,\left[\frac{\mathrm{t_{tp}}}{\mathrm{t}}\right]^2\,\mathrm{Exp}\left\{-\left[\mathrm{t_{tp}/t}\right]^{\mathrm{n}-1}\right\}\,. \tag{33}$$

Let the peak γ-ray energy at a fixed time during a GRB pulse be defined as $\mathrm{E_p^\gamma(t)} \equiv \max\left[\mathrm{E^2\,dI_\gamma/dE\,dt}\right]$. Its value is $\mathrm{E_p^\gamma(t)} \simeq 3.92\,\delta\,\mathrm{T[t]}/(1+\mathrm{z})$, so that, for t near or after $\mathrm{t_{tp}}$:

$$\mathrm{E_p^\gamma(t)} \simeq \mathrm{E_p^\gamma(t_{tp})}\,\Theta[\mathrm{t}]\,\frac{\mathrm{t_{tp}}}{\mathrm{t}}\,. \tag{34}$$

The total "isotropic" energy of a GRB pulse —deduced from its observed fluence assuming an isotropic emission— can be deduced from Eq. (18), to be:

$$\mathrm{E_{iso}} = \frac{4\,\pi\,\mathrm{D_L^2\,F}}{1+\mathrm{z}} \simeq \mathrm{E_{pulse}^{rest}}\,\delta^3\,. \tag{35}$$

If CBs were "standard candles" with fixed mass, energy and velocity of expansion, and if all SN shells had the same mass, radius and density distribution, all differences between GRB pulses would result from their different distances and angles of observation. For such standard candles it follows from Eqs.(3-5,35) that the observed durations (half widths at half maximum) of the photon intensity and of the energy flux density ($\Delta\mathrm{t_I}$ and $\Delta\mathrm{t_F}$), their peak values ($\mathrm{N_p}$ and $\mathrm{F_p}$), and the peak energy ($\mathrm{E_p^\gamma}$) in a single GRB pulse are roughly correlated to the total "observed" isotropic energy ($\mathrm{E_{iso}}$) as follows:

$$\Delta\mathrm{t_I} \propto (1+\mathrm{z})\,[\mathrm{E_{iso}}]^{-1/3}\,, \tag{36}$$

$$\Delta\mathrm{t_F} \propto (1+\mathrm{z})\,[\mathrm{E_{iso}}]^{-1/3}, \tag{37}$$

$$\mathrm{N_p} \propto \mathrm{E_{iso}}, \tag{38}$$

$$\mathrm{F_p} \propto [\mathrm{E_{iso}}]^{4/3}\,(1+\mathrm{z})^{-1}\,, \tag{39}$$

$$\mathrm{E_p^\gamma} \propto [\mathrm{E_{iso}}]^{1/3}\,(1+\mathrm{z})^{-1}\,. \tag{40}$$

These approximate correlations can be tested using the sample of 15 GRBs with known redshifts. Because of the strong dependence of the CB pulses on the Doppler factor and their much weaker dependence on the other parameters, they may be approximately satisfied (see, e.g. Plaga 2000) in spite of the fact that CBs and SN shells are likely to be sufficiently varied not to result in standard candles.

Within the standard-candle approximation there is also a simple correlation between the rate and the fluence of GRBs. For the region of the universe that is close enough to us to be approximately homogeneous and Euclidean, Eq.(18) implies that $\mathrm{F} = \mathrm{E_{rest}^{pulse}}\,\delta^3/(4\,\pi\,\mathrm{D}^2)$. If CBs were *stationary*, the corresponding rate of GRB pulses with fluence larger than a given $\mathrm{F_0}$ would satisfy the well known relation:

$$\dot{\mathrm{N}}(>\mathrm{F_0}) \simeq \dot{\mathrm{n}}_{\mathrm{CB}}\,\frac{4\,\pi}{3}\,\left[\frac{\mathrm{E_{rest}^{pulse}}}{4\,\pi\,\mathrm{F_0}}\right]^{\frac{3}{2}} \propto \mathrm{F_0^{-3/2}}, \tag{41}$$

where $\dot{\mathrm{n}}_{\mathrm{CB}}$ is the mean production rate of CBs per unit volume. For our highly relativistic CBs, whose "isotropic" energy is multiplied by the factor δ^3, Eq.(41) is modified to:

$$\dot{\mathrm{N}}(>\mathrm{F_0}) \simeq \frac{3}{7}\,\frac{2^{\frac{7}{2}}}{\gamma^2}\,\dot{\mathrm{n}}_{\mathrm{CB}}\,\frac{4\,\pi}{3}\,\left[\frac{\gamma^3\,\mathrm{E_{rest}^{pulse}}}{4\,\pi\,\mathrm{F_0}}\right]^{\frac{3}{2}} \propto \mathrm{F_0^{-3/2}}, \tag{42}$$

yielding the same rate-to-fluence relation. The same power-law scaling is obtained for the relation between the

rate and the peak-energy density-flux from CBs. Both relations should be approximately satisfied by very bright (relatively nearby) GRBs.

For distant GRBs the above relations are sensitive to the cosmological model, to the not-well-determined SN- (or star-formation) rate and to the strong selection effect favouring observations of distant GRBs with large γ and a small viewing angle θ, and a correspondingly large Doppler-enhancement δ. Because of this, we do not discuss here the rate-to-fluence relation for faint GRBs (Yi, 1994; Plaga 2000).

7. Predictions of the Cannonball Model

Some common properties of GRB pulses (for detailed light curves see Kippen 2000; Mallozzi 2000) are observed to be:

- (a) The GRB fluences, integrated in energy and time, lie within one or two orders of magnitude above or below 10^{-5} erg/cm^2 (see, e.g., Paciesas et al. 1999).
- (b) Individual pulses are narrower in time, the higher the energy interval of their individual photons (see, e.g., Fenimore et al. 1995).
- (c) Individual pulses rise and peak at earlier time, the higher the energy interval of their individual photons (see, e.g., Norris et al. 1999; Wu and Fenimore 2000)
- (d) Individual pulses have smaller photon energies, the later the time-interval of observation (see, e.g., Preece et al. 1998) .
- (e) The energy spectrum of GRBs, or of their individual pulses, if plotted as $E^2\,dN/dE$, rises with energy as E^α, with $\alpha \sim 1$, has a broad peak at E $\sim$ 0.1 to 1 MeV, and decreases thereafter (see, e.g., Preece 2000).
- (f) Most GRBs consist of pulses whose time-behaviour is a fast rise followed by an approximately exponential decay: a "FRED" shape. Some GRBs have non-FRED, roughly time-symmetric pulses (see e.g., Fenimore et al. 1995 and references therein) The overwhelming majority of GRBs are either made of FRED or non-FRED pulses: there are no GRBs with mixed pulse-shapes.

All of the above items are properties of the CB model.

In Fig.(1) we illustrate item (a) by plotting the total fluence, estimated with use of Eq.(18) and varying one parameter at a time. Naturally, the highest sensitivity is that to the viewing angle θ, followed by that to E_{CB} and z. The remaining itemized GRB properties all follow from Eq.(27); items (b,c,d) are even apparent in the simplified Eq.(31) for the time and energy dependence of the γ-ray flux. In Fig.(2) we illustrate items (b) and (c) by plotting Eq.(27) at three fixed γ-ray energies, for all parameters fixed at the reference values of Table I. In Fig.(3) we similarly illustrate item (d) in a plot at three different times, multiples of the time of shell transparency. Item (e) is illustrated in Fig.(4) where we plot $E^2\,dN/dE$, obtained by integrating Eq.(27) over all times; the figure also reports the sensitivity to various parameters, by modifying them, one at a time, relative to the reference parameters. In Fig.(5) we illustrate item (f) by plotting dN/dt, obtained by integrating Eq.(27) over all energies above 30 keV. Once again, we vary reference parameters as in Fig.(4). Redshift not being a free parameter specific to our model, we separately illustrate in Fig.(6) the z-dependence of the time-integrated and energy-integrated versions of Eq.(27).

A look at Figs.(5) and (6) reveals that, for the parameter ranges explored therein, all the predicted GRB-pulse shapes are FREDs and are relatively short in time (fractions of a second). Yet, these are not general predictions of Eq.(27). It is, for instance, quite conceivable that the ejection of a shell in a SN explosion be due to one or various CBs emitted immediately after core implosion: the shock wave induced by their passage through the outer shells of the star would trigger their ejection. In that case the outgoing shell would be quite disrupted in the "polar" directions in which later CBs would result in a GRB. It is also possible that a GRB be due to the passage of CBs through material expelled by a parent-star's wind, as opposed to the SN shell. In both cases, the density profile of the matter traversed by a GRB may be very different from that described by a large index n $\sim$ 4 to 8 in Eq.(10), indicated by observations of complete SN shells, not of their small polar regions. In Fig.(7) we illustrate these points by plotting dN/dt for n = 2, 3, with the rest of the parameters at their reference values, and we also give an example with n = 6 and a very large viewing angle $\theta = 20/\gamma_{\rm out}$. All three of these time-profiles are quite symmetrical non-FREDs and have durations in the few-second range (it is also possible to generate long-duration FREDs, as we shall see below in the specific case of GRB 980425).

In Fig.(8) we plot a GRB with 6 CBs, shot at random times in a 1.5 s interval and with random values of E_{CB} within a factor of three of our reference value. All other parameters in this figure, but the SN-shell density-profile index n, have their reference values: the only difference between Fig.(8a) and Fig.(8b) is that n = 8 in the former, n = 4 in the latter. These figures illustrate the obvious fact that the correspondence between CBs and observed pulses need not be biunivocal: a CB produces a GRB pulse, but an observed pulse can be due to a superposition of CB subpulses. Notice that this is also a way to obtain pulses that are very wide, or do not have FRED- or symmetrical shapes.

8. Brief comparison to some data

Comparing a GRB theory with specific GRBs is a tricky task, for an obvious reason: GRBs being all different, one may be tempted to choose GRBs that fit the theory, rather than doing the opposite. In this Section we investigate three GRBs with measured redshifts. Of this ensemble, we use the highest fluence event (Briggs et al 1999) GRB 990123 (z = 1.6), to analize the energy distribution; we use GRB 980425 (Kippen 2000), whose redshift (Galama

et al. 1998) is by far the smallest (z = 0.0085) and yet has a conventional fluence (Kippen et al. 1998), to study the time-dependence of its single pulse; finally, we use GRB 990712 (z = 0.4315) to study the correlation between the γ-ray energy- and time-distributions (Mallozzi 2000) and to expose the limitations of the CB model in its present simple form.

8.1. Energy dependence

The predicted energy spectrum of a GRB is obtained by integrating Eq.(27) over all times. The resulting flux distribution and the same result weighed with E^2 are compared with the GRB 990123 data in Fig.(9). The parameters used are $\overline{\beta}_{\rm in} = 1/4$, $\overline{\beta}_{\rm out} = 1$, $\overline{\rm M}_{\rm S} = 1/5$, $\overline{\rm R}_{\rm S} = 1/2$, $\overline{\rm E}_{\rm CB} = 20$, $\overline{\gamma}_{\rm out} = 1.5$, $\overline{\theta}_{\rm S} = 1.46$, n = 6 and z = 1.6. The value of $E_{\rm CB}$ may look large, but this is a multiple-pulse GRB and the energy distribution is integrated over all pulses: $\overline{\rm E}_{\rm CB} = 20$ corresponds only to twice our reference value for $E_{\rm jet}$. For these parameters the GRB fluence, as estimated via Eq.(18), is the observed $26.5\ 10^{-5}$ erg cm^{-2}. Since the shape of the energy distribution is insensitive to the various parameters, as seen in Fig.(4), it is easy to find many parameter ensembles that result in the same prediction: the energy distribution by itself is not a good observable to constrain the input, but is, on the other hand, a solid test of the model.

The shape of the energy spectrum dN/dE of Fig.(9a) can be easily understood. At the lower energies, the $\sim$1/E behaviour is the result of integration over thermal spectra with temperatures that decrease with time, see Fig.(3). The abrupt decrease of dN/dE at the higher energies reflects the input thermal spectrum at the time and temperature at which the SN shell starts to become transparent.

The comparison made in Fig.(9) is quite satisfactory, particularly if one realises that many of the higher-energy data are but upper limits. In making this figure we used the thermal distribution of Eq.(25), and the fact that at the higher energies the theory may undershoot relative to the data is to be expected. Indeed, the CB, in its rest system, is subject to a flux of high energy nuclei and electrons. While the electrons are being thermalized, they should contribute a nonthermal high-energy tail of photons emitted via the "free-free" process. Such a power-law tail in an otherwise approximately-thermal emission is observed from young supernova remnants (see, e.g., Dyer et al. 2000) and clusters of galaxies (e.g., Fusco-Femiano et al. 1999; Rephaeli et al., 1999; Fusco-Femiano et al., 2000), both of which are systems wherein a dilute plasma at a temperature of $\mathcal{O}$(1 keV) is exposed to a flux of high energy cosmic rays.

8.2. Time dependence

In Fig.(10) we compare the single-pulse light curve of GRB 980425 (Kippen 2000) with the CB theory, obtained by integrating Eq.(27) over energy, in the 50-300 keV domain. The parameters used are $\overline{\beta}_{\rm in} = 1/3$, $\overline{\beta}_{\rm out} = 1/2$, $\overline{\rm M}_{\rm S} = 1$, $\overline{\rm R}_{\rm S} = 2$, $\overline{\rm E}_{\rm CB} = 10$ (corresponding to our reference jet energy in a single pulse), $\overline{\gamma}_{\rm out} = 1/3$, $\overline{\theta}_{\rm S} = 60$, n = 8 and z = 0.0085. For these parameters the GRB fluence, as estimated via Eq.(18), is the observed 0.44×10^{-5} erg cm^{-2}. Notice that the value used for the viewing angle θ is very large: this is the explanation (Dar and De Rújula 2000a) why this particular GRB has a normal fluence, in spite of how close its progenitor (SN 1998bw) is to us.

The comparison made in Fig.(10) is entirely satisfactory. The parameter domain giving rise to a light curve with a particular shape, height and width is much more restricted than the corresponding domain for an energy distribution. Yet, we cannot entirely trust the approximate parameter values thus extracted, for the reasons to be discussed in the next two subsections.

8.3. The time-energy correlation

In Fig.(11) we compare the single-pulse light curves of GRB 990712 (Mallozzi 2000) with the CB theory (the continuous red curves), obtained by integrating Eq.(27) over energy, in the same domains as the data: 20-50 keV (BATSE channel 1.1), 50-100 keV (2.2), 100-300 keV (3.3) and > 300 keV (4.4). The parameters used are $\overline{\beta}_{\rm in} = 1$, $\overline{\beta}_{\rm out} = 1/3$, $\overline{\rm M}_{\rm S} = 1/4$, $\overline{\rm R}_{\rm S} = 3$, $\overline{\rm E}_{\rm CB} = 50$ (corresponding to five times our reference jet energy in a single pulse), $\overline{\gamma}_{\rm out} = 1/5$, $\overline{\theta}_{\rm S} = 1/2$, n = 3, and z = 0.4315.

The comparison made in Fig.(11) is rather unsatisfactory, in that the correlation between energy-interval and pulse-width is weaker in the observations than it is in the predictions. The theoretical correlation, for a thermal input spectrum, is roughly that implied by the simplified expression Eq.(31), that is Δt ΔE $\sim$ H, in an obvious notation. The dashed blue curves in Fig.(11) correspond to a modified input in which we have assumed that the CB cooling (as discussed in Section 8.5) may be not be linear in time, but closer to quadratic, so that $\Delta t \propto 1/\sqrt{\Delta E}$. This modification goes in the right direction, but it is still not entirely satisfactory. We have not yet investigated in detail how a deviation from an input thermal spectrum at high energies –that we discussed in Section 8.1 in commenting Fig.(9)– affects the time-energy correlation. But, since a non-thermal high-energy tail broadens the energy-distribution at all times, it ought to weaken even further the time-energy correlation, as required.

We have studied the time-energy correlation for other single-pulse GRBs, such as 981022, 981221 and 990102. They all have a weaker energy-interval to pulse-width correlation than our model predicts, though the problem is most acute for GRB 990712, that we have thus chosen to expose the limitations of the CB model in its current formulation.

8.4. Lessons from the comparison with data

We conclude from our study of the general properties of GRBs in Section 7, and from the three comparisons with data in Section 8, that we may have deliniated the correct overall energetics of the collision of the CB with the SN shell, but our treatment of the time evolution of the processes of heating and cooling is oversimplified. A posteriori, there are many obvious reasons why this ought to be the case: the front of the CB is no doubt at a higher temperature than its bulk, since the CB is many collision-lengths long and is dominantly heated at the front: only muons and their decay electrons –but not photons from π^0 decay– heat the bulk. The process is not a sudden heating followed by continuous cooling, as we assumed. We have included cooling by expansion, but not by emission from the CB's surface. We have assumed a constant expansion velocity, and not attempted to compute an actual expansion history from plasma dynamics. The CB may not have a constant density, it may even be a discontinuous ball of "shrapnel". Etc. etc.

8.5. An alternative simplified model

The six general properties of GRBs discussed in Section 7 ought to be quite independent of the complex details of the CB's collision with the SN shell, since they only capitalize on the overall energetics and on the fact that, as it reaches the transparent outskirts of the SN shell, the CB is cooling by radiation and expansion. We illustrate this point by sketching an alternative model of CB heating and cooling, a simplified "surface" model that is in some sense the extreme opposite to the simplified "volume" model we have discussed in detail. To lighten the discussion, in all numerical results in this chapter we fix the parameters to their reference values of Table I.

In its rest frame, the front surface of the CB is bombarded by the nuclei of the SN shell, which have an energy $m_p\,c^2\,\gamma \sim 1$ TeV per nucleon, roughly 1/3 of which (from $\pi^0 \to \gamma\gamma$ decays) is converted into these γ-rays within $X_p \approx m_p/\sigma_{in}(pp) \approx 50\,g\,cm^{-2}$, where $\sigma_{in}(pp)$ is the nucleon-nucleon inelastic cross section. These high energy photons initiate electromagnetic cascades that eventually convert their energy to thermal energy within the CB. The radiation length of high energy γ's in hydrogenic plasma, dominated by $e^+\,e^-$ pair production, is $X_{\gamma e} \simeq 63$ g cm^{-2}, comparable to X_p. The radiation length of thermalized photons in a hydrogenic plasma is $X_\gamma^{ion} \approx m_p/\sigma_T \approx 2.6$ g cm^{-2}.

Assume that the quasi-thermal emission rate from the CB, within X_γ^{ion} from its surface, is in dynamical equilibrium with the fraction of energy deposited by the CB's collision with the SN shell in that outer layer. The temperature of the CB's front is then roughly given by:

$$T(x) \simeq \left[\frac{(n-1)\,X_\gamma\,m_p\,c^3[\gamma(x)]^2\,\sigma_{in}(pp)}{6\,\sigma\,x_{tp}\,X_{\gamma e}\,\sigma_T^2}\right]^{\frac{1}{4}}\left[\frac{x}{x_{tp}}\right]^{-\frac{n}{4}}, \quad (43)$$

where $\gamma(x)$ is a function that decreases monotonically from γ_{in} to γ_{out}. Remarkably, only the Lorentz factor of the CBs, but neither their mass nor their energy, appear in the above expression, except for the fact that, for the result to be correct, they must be large enough for the CB to pierce the SN shell and remain relativistic.

For $n = 8$ the value of x_{tp} is $\approx 3\,R_S$, and, for t close to t_{tp} or later:

$$T(t) \simeq 0.16\,keV\left[\frac{t_{tp}}{t}\right]^2\left[\frac{\gamma(t)}{10^3}\right]^{\frac{1}{2}}. \quad (44)$$

At the time of transparency this is quite comparable to the result of combining Eqs.(21) and (22). However, only for $n = 4$ does the temperature decrease approximately as $1/t$. For $n > 4$ it diminishes faster than $1/t$ and for $n = 8$ it decreases faster than $1/t^2$, the "faster" being due, in both cases, to the effect of a decreasing $\gamma(t)$. For an exact $1/t^2$ behaviour the pulse width narrows with time as $\Delta t \propto E^{-0.5}$ and, as we have also seen in Section 8.3, this goes in the direction of improving the predicted time-energy correlation. In fact, Fenimore et al. (1995) found, from a large sample of GRB pulses, that $\Delta t \propto E^{-0.46}$.

The total radiated energy, in the CB rest frame, is roughly the thermal energy deposition within one radiation length from its front surface. After attenuation in the SN shell, it reduces to:

$$E_{pulse}^{rest} \approx \frac{\sigma_{in}(pp)\,\pi\,[R_{CB}^{tp}]^2\,\bar{X}_\gamma\,m_p\,c^2\,\gamma(t)}{3\,X_{\gamma e}\,\sigma_T^2}, \quad (45)$$

where $\bar{X}_\gamma$ is the radiation length in the obscuring shell averaged over the black body spectrum. For a typical γ-ray peak energy of $E_p \sim 1$ MeV in the SN rest frame, $\bar{X}_\gamma \simeq 10$ g cm^{-2}. Consequently, the CB's radius at transparency is $R_{CB}^{tp} = 4\times10^{11}$ cm and $E_{pulse}^{rest} \sim 3\times10^{45}$ erg, for $\gamma(t) \sim 10^3$. This is consistent with the results in Eqs.(17), implying that the predicted fluences in the surface-heating and volume-heating models are quite similar. The fact that the characteristic temperatures of the volume-heating and the surface-heating models around the time of transparency are also similar means that their predicted GRB individual-photon energies are comparable and both in agreement with the GRB observations.

9. Conclusions

In a previous paper (Dar and De Rújula 2000a) we have argued that the CB model provides a very good description of GRB afterglows, including those whose light curve is seen to rise before it drops, as is the case for GRB 970508. There we also contended that, in the case of GRB 980425, the model provides a strong motivation for the search of the superluminal motion of the afterglow-emitting CB, relative to the associated supernova: SN1998bw. This would be a decisive signature for highly relativistic cannonballs,

as opposed to conically spreading jets. We plan to discuss in future work other important signatures of the CB model: high energy neutrinos and photons during the GRB, flare up and X-ray lines in its early afterglow.

In this paper we have demonstrated that the CB model explains the fluence and energy spectrum of GRBs, as well as the characteristic properties of their light curves. The detailed heating, expanding and cooling of the CB —as it hits and sweeps up the SN shell— we have treated only in a simplified fashion. As a consequence, the model in its present form does not provide a completely satisfactory quantitative description of the time-energy correlation. We may not have completely untied the perduring Gordian knot of the GRB conundrum, but we have argued that we have sliced it open.

Aknowledgements We are indebted to Rainer Plaga for interesting discussions. This work was supported in part by the Fund for Promotion Of Research At The Technion.

Parameter	Symbol	Value
SN-shell's mass	M_S	10 $M_\odot$
SN-shell's radius	R_S	2.6×10^{14} cm
SN-shell's density index	n	8
Outgoing Lorentz factor	γ_{out}	10^3
CB's viewing angle	θ	10^{-3}
CB's energy	E_{CB}	10^{52} erg
Initial v_T/c of expansion	β_{in}	$1/(10\sqrt{3})$
Final v_T/c of expansion	β_{out}	$1/\sqrt{3}$
Redshift	z	1

Table I. List of the "reference" values of various parameters. In the text a barred parameter means its actual value divided by its reference value, so that, for instance, $\overline{M}_S = 1/2$ means the actual mass of the SN shell is taken to be 5 $M_\odot$.

References

Belloni T., et al., 1997, ApJ 479, 145
Blandford R.D., Znajek R.L., 1977, MNRAS 179, 433
Bridle A. 2000, http://www.cv.nrao.edu/∼abridle/radiogal.htm
Briggs M.S., et al., 1999, ApJ 524, 82
Cen R., 1999, ApJ 524, 51
Celotti A., et al. 1997 MNRAS 286, 415
Costa E., et al., 1997, Nature 387, 783
Dar A., 1998, ApJ 500, L93
Dar A., 1999, A&A 138S, 505
Dar A., De Rújula, A., 2000a, A&A accepted (astro-ph/0008474)
Dar A., De Rújula, A., 2000b, to be submitted
Dar A., De Rújula, A., 2000c, to be submitted
Dar A., De Rújula, A., 2000d, astro-ph/0002014, submitted to MNRAS
Dar A., Plaga R., 1999, A&A 349, 259
De Rújula A., 1987, Phys. Lett. 193, 514
Dyer K.K., et al., 2000, astro-ph/0011578
Fenimore E.E., Ramirez-Ruiz E., 2000, astro-ph/0004176
Fenimore E.E., et al., 1995, ApJ 448, L101
Fusco-Femiano R., et al., 1999, ApJ, 513, L21
Fusco-Femiano R., et al., 2000, astro-ph/0003141
Galama T.J., et al., 1998, Nature 395, 670
Ghisellini G., 2000, astro-ph/0012125
Goodman J., Dar, A., Nussinov, S., 1987, ApJ 314, L7
Groom D.E., et al., 2000, *Review of Particle Physics*, Eur. Phys. J. C15, 1
Kippen R.M., et al., 1998, GCN 67
Kippen R.M., 2000, http://www.batse.msfc.nasa.gov/∼kippen/batserbr/brbr_obs.html
Lyne A.G., Lorimer, D.R., 1994, Nature 369, 127
Metzger M.R., et al., 1997, Nature 387, 878
MacFadyen A.I., Woosley S.E., 1999, ApJ 524, 168
Mallozzi, R.S., 2000, http://www.batse.msfc.nasa.gov/batse/
Margon B.A., 1984, ARA&A 22, 507
Meszaros P., Rees M.J., 1992, MNRAS 257, 29
Meszaros P., Rees M.J., 1997, ApJ 482, L29
Mirabel I.F., Rodriguez, L.F., 1994, Nature 371, 46
Mirabel, I.F., Rodriguez, L.F., 1999a, ARA&A 37, 409
Mirabel, I.F., Rodriguez, L.F. 1999b, astro-ph/9902062
Norris J.P., et al., 1999, astro-ph/9903233
Nakamura T. et al., 2000, astro-ph/0007010
Paciesas W.S., et al., 1999, ApJS 122, 465)
Paczynski B., 1986, ApJ 308, L43
Paczynski B., 1998, ApJ 494, L45
Plaga R., 2000, astro-ph/001206
Preece R.D., 2000, ApJS 126, 19
Preece R.D., et al., 1998, ApJ 496, 849
Rephaeli Y., et al., 1999, ApJ 511 L21
Rodriguez L.F., Mirabel, I.F., 1999, ApJ 511, 398
Shaviv N.J., Dar A., 1995, ApJ 447, 863
Tingay S.J., et al., 1995, Nature 374, 141
van Paradijs J., et al., 1997, Nature 386, 686
Wilson A.S., et al., 2000, astro-ph/0008467
Woosley S.E., 1993, ApJ, 405, 273
Woosley S.E., 1999, in the *Fifth Huntsville Conference on Gamma-Ray Bursts*, eds. R. M. Kippen, R.S. Mallozzi, & V. Connaughton, AIP
Woosley S.E., MacFadyen, A.I., 1999, A&AS 138, 499
Wu B., Fenimore L., 2000, ApJ 535, L29
Yi I., 1994, ApJ 431, 543

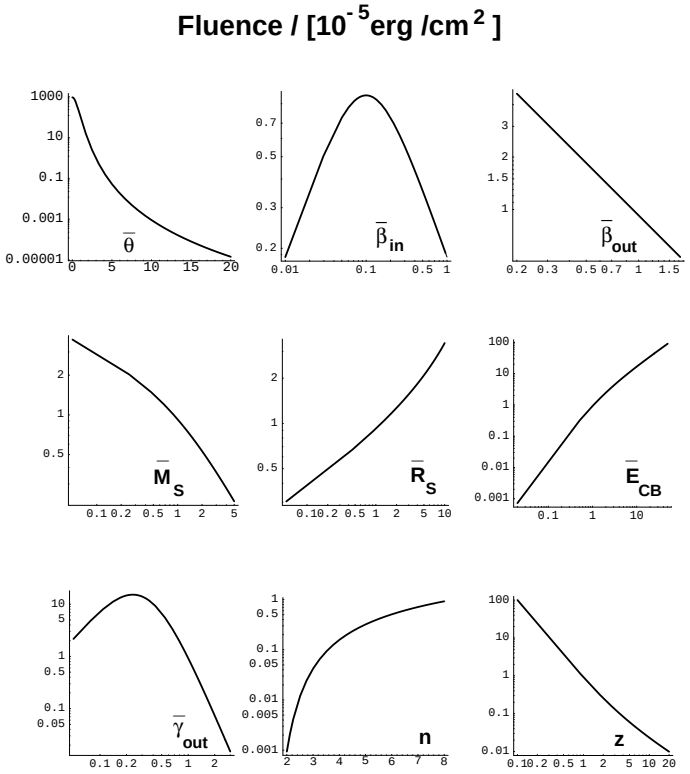

FIG. 1.— Fluence as a function of various parameters, in units of 10^{-5} erg/cm^2. The parameters θ through $\gamma_{\rm out}$ are in units of their reference values of Table I, thus the barred notation. The index n and the redshift z are not rescaled. All parameters not being varied are fixed at their reference values of Table I, but for θ, fixed at a "typical" $\overline{\theta} = 3$.

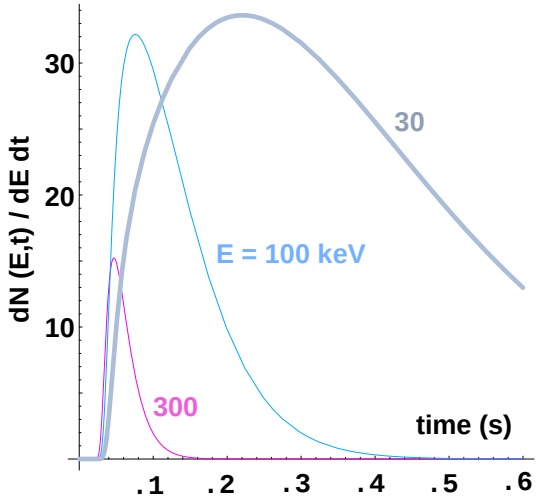

FIG. 2.— GRB-pulse shape as a function of time, at various fixed γ-energies.

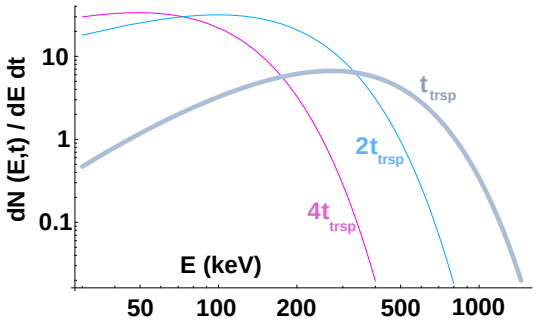

FIG. 3.— GRB γ-energy distributions, at various fixed times, multiples of the (observer's) time at which the SN-shell becomes transparent.

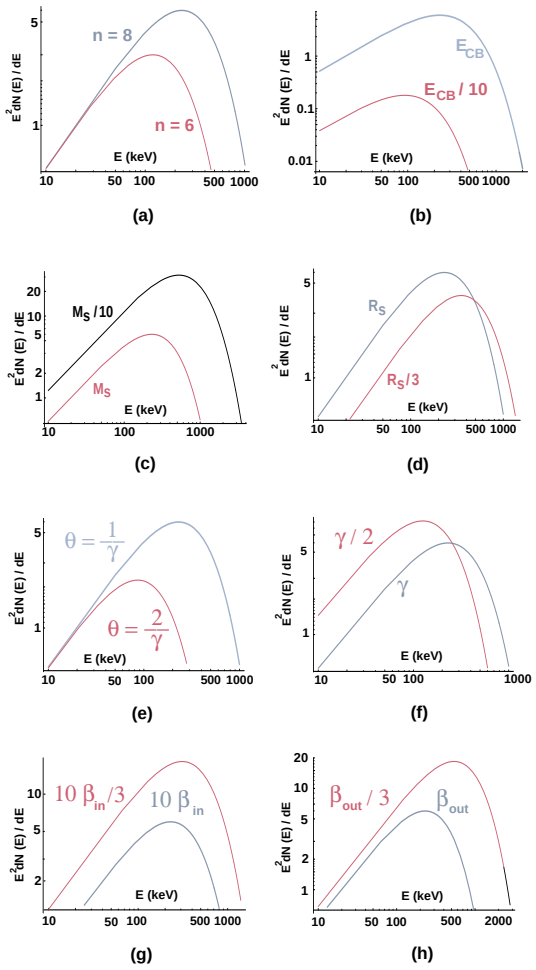

FIG. 4.— Time-integrated E^2 dN/dE distributions, illustrating the sensitivity to one parameter at a time. The absolute vertical scale is arbitrary, but the relative scales are not. All parameters not mentioned in each subfigure are kept at the reference values of Table I (but for $\beta_{\rm in}$, which is fixed at $1/\sqrt{3}$). Notice that the shape of the energy distribution is always the same, irrespective of the parameter values.

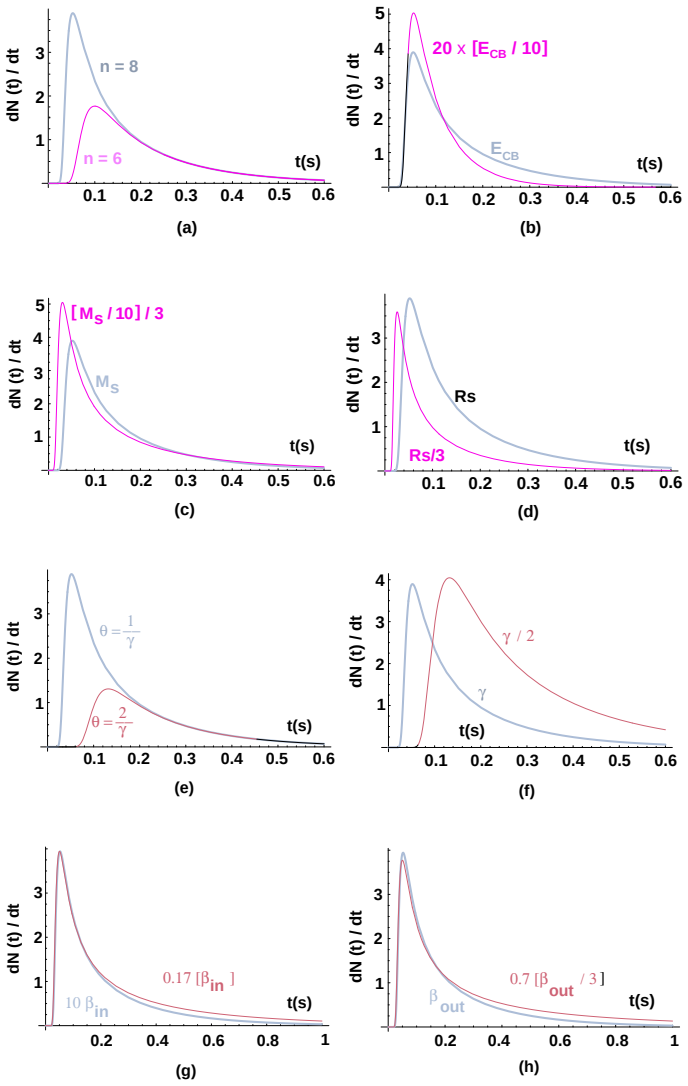

FIG. 5.— Time distribution dN/dt of a single GRB pulse, integrated for all E > 30 keV. The absolute vertical scale is arbitrary, but the relative scales are not. All parameters not mentioned in each subfigure are kept at the reference values of Table I (but for $\beta_{\rm in}$, which is fixed at $1/\sqrt{3}$). For ease of comparison, in some subfigures, a curve has been rescaled, e.g. in (b) the result for an input $E_{\rm CB}/10$ has been multiplied by 20.

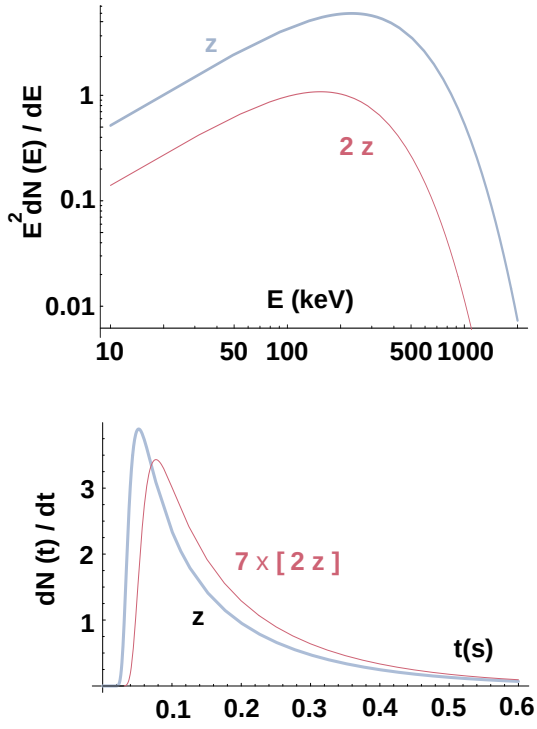

FIG. 6.— Illustration of the sensitivity to redshift, z, of the energy-and time-distributions in a GRB pulse.

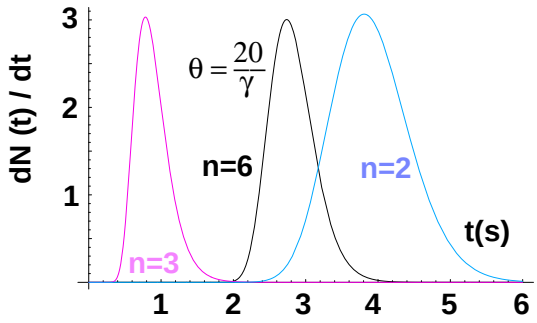

FIG. 7.— Examples of parameter values that give rise to non-FRED pulse shapes. The individual vertical scales are chosen for ease on comparison. All parameters not mentioned are as in Table I.

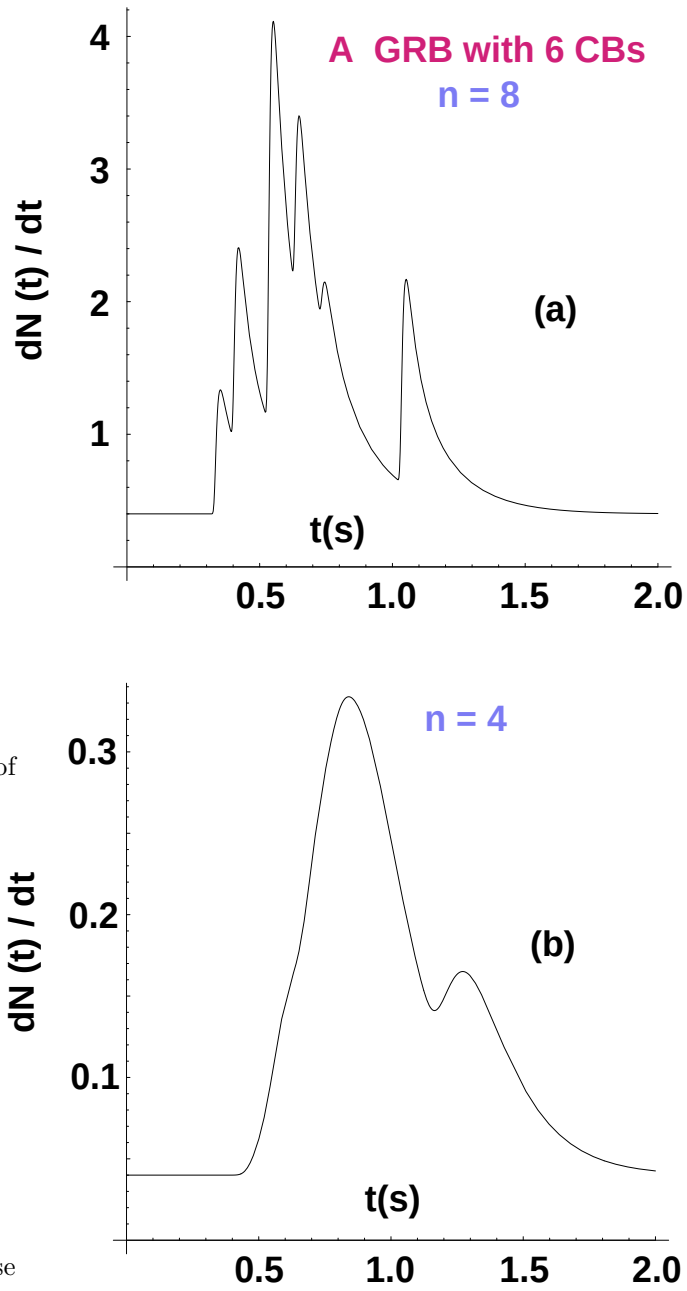

FIG. 8.— "Synthetic" GRB light curves, generated by shooting six CBs at random in a 1.5 s time-interval, and with random values of E_{CB} within a factor of three of our reference value. The only difference between (a) and (b) is that n = 8 in (a), while n = 4 in (b). All other parameters in this figure have their reference values. The figure illustrates how a CB produces a GRB pulse, but a GRB-pulse may not correspond to a single CB.

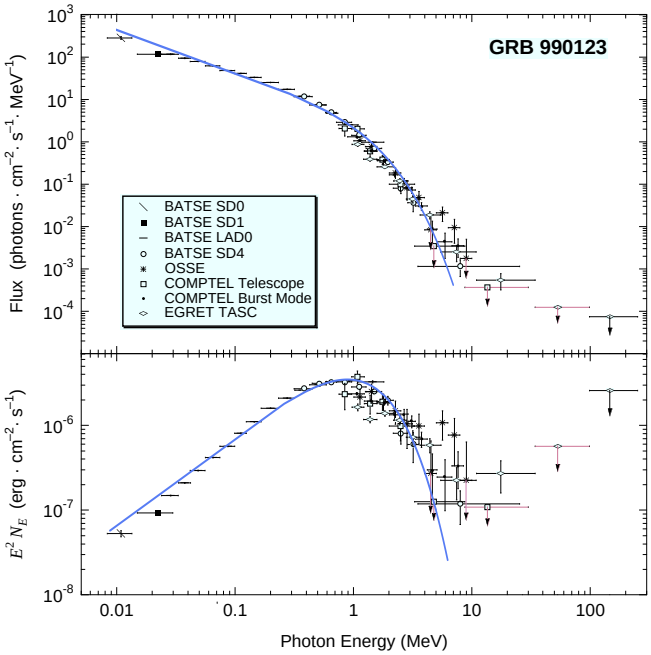

FIG. 9.— Comparison of theory and observation for the time-integrated energy distributions dN/dE and E^2 dN/dE, in the case of GRB 990123. Notice that many experimental points at the higher energies are only upper limits.

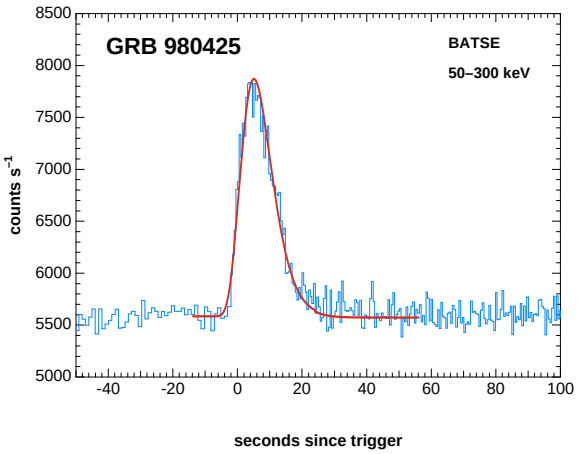

FIG. 10.— Comparison of theory and observation for the light curve of GRB 980425, in the 50-300 keV energy interval.

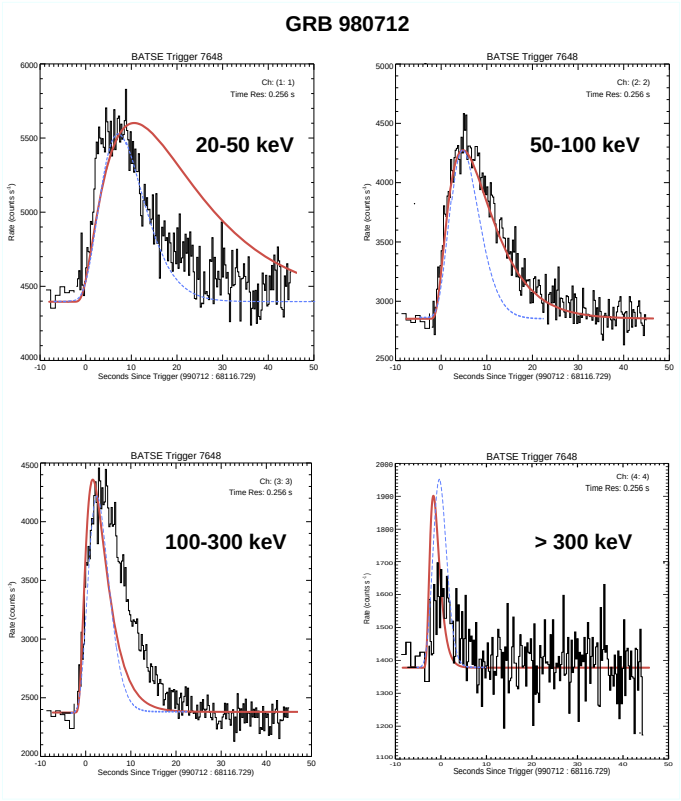

FIG. 11.— Comparison of theory and observations for the light curve of GRB 980712, in various BATSE energy intervals.